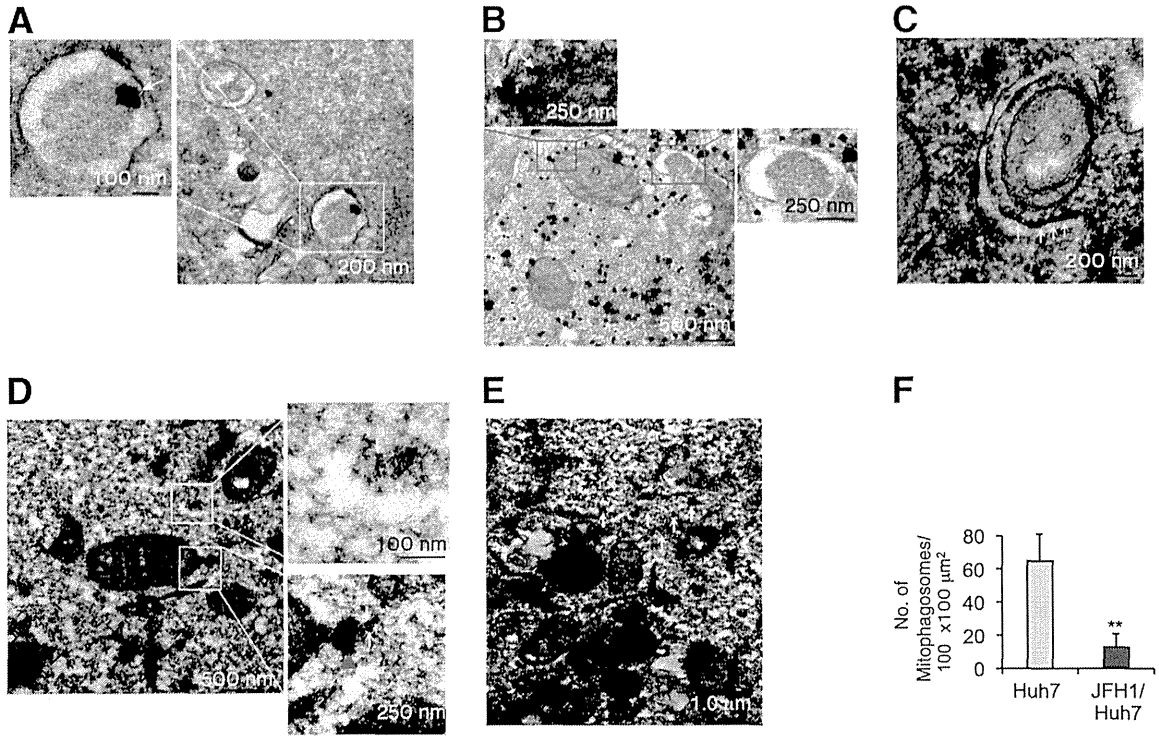

Figure 6 Electron microscopy of Huh7 cells and JFH1-Huh7 cells after carbonyl cyanide *m*-chlorophenylhydrazone (CCCP) treatment. **A—E:** Electron micrographs. **Boxed areas** are enlarged on left (Huh7 cell; **A**), above and on the right (Huh7 cell; **B**), and on the right (JFH1-Huh7 cell; **D**). The **arrows** indicate Parkin labeled with gold on the mitochondrial outer membrane (**A** and **B**), LC3 protein labeled with diaminobenzidine (DAB) on elongating isolation membrane that sequesters a single mitochondrion (Huh7 cells; **C**), Parkin core (**D**), and Parkin labeled with gold (JFH1-Huh7 cell; **E**). The **arrowheads** indicate Parkin labeled with gold (**B**) and HCV core (**D**). **F:** The number of mitophagosomes per 100 × 100 μm^2 was calculated for four randomly selected views. $^{**}P < 0.01$.

determined whether the HCV core protein binds to the region that includes lysine (K) 211 in the RING0 domain, the specific interaction of Parkin 1 to 215 with the HCV core protein raises the possibility that the core protein inhibits Parkin translocation to the mitochondria by affecting lysine 211.

After we confirmed the specific interaction between the HCV core protein and Parkin, we investigated whether Parkin affects HCV replication to investigate the functional role of the interaction between both proteins in the HCV infectious process. Parkin silencing significantly inhibited HCV replication, as indicated by a decrease in HCV core protein expression, but did not affect HCV core mRNA levels (Figure 5E). These results suggest that the association of the HCV core protein with Parkin plays a functional role in HCV propagation, although further studies are required to clarify the mechanisms.

Suppressed Ubiquitination of the Mitochondrial Outer Membrane Protein VDAC1

The next step in mitophagy after Parkin translocation to the mitochondria is the ubiquitination of mitochondrial outer membrane proteins.[13,16] Coimmunoprecipitation experiments revealed that various sizes of ubiquitinated VDAC1 species in the mitochondrial outer membrane[13] were present after CCCP treatment in Huh7 cells but not in JFH1-Huh7 cells (Figure 5F). Western blot analysis of VDAC1 immunoprecipitates revealed various sizes of VDAC1 species after CCCP treatment in Huh7 cells but not in JFH1-Huh7 cells (Figure 5F). The autophagic adaptor p62 aggregates ubiquitinated proteins by polymerizing with other p62 molecules.[13] Similarly, coimmunoprecipitation experiments revealed that CCCP treatment induced various sizes of ubiquitinated p62 species in Huh7 cells but not in JFH1-Huh7 cells (Figure 5G). These results suggest that HCV infection inhibited the Parkin-induced ubiquitination of the depolarized mitochondria.

Suppressed Mitophagosome Formation

During mitophagy, the isolation membrane sequesters a single mitochondrion or a cluster of mitochondria to form an autophagosome (mitophagosome). A single mitochondrion with Parkin on its outer membrane was sequestered by the isolation membrane after CCCP treatment in Huh7 cells (Figure 6A). Parkin in close proximity to the mitochondria and association of Parkin with mitochondrial outer membrane were observed more frequently in Huh7 cells than in JFH1-Huh7 cells (Figure 6, B, D, and E). In addition, LC3 was present on elongating isolation membrane that sequesters a single mitochondrion after CCCP treatment in Huh7 cells (Figure 6C). The number of mitophagosomes, calculated as the number of autophagosomes that contain

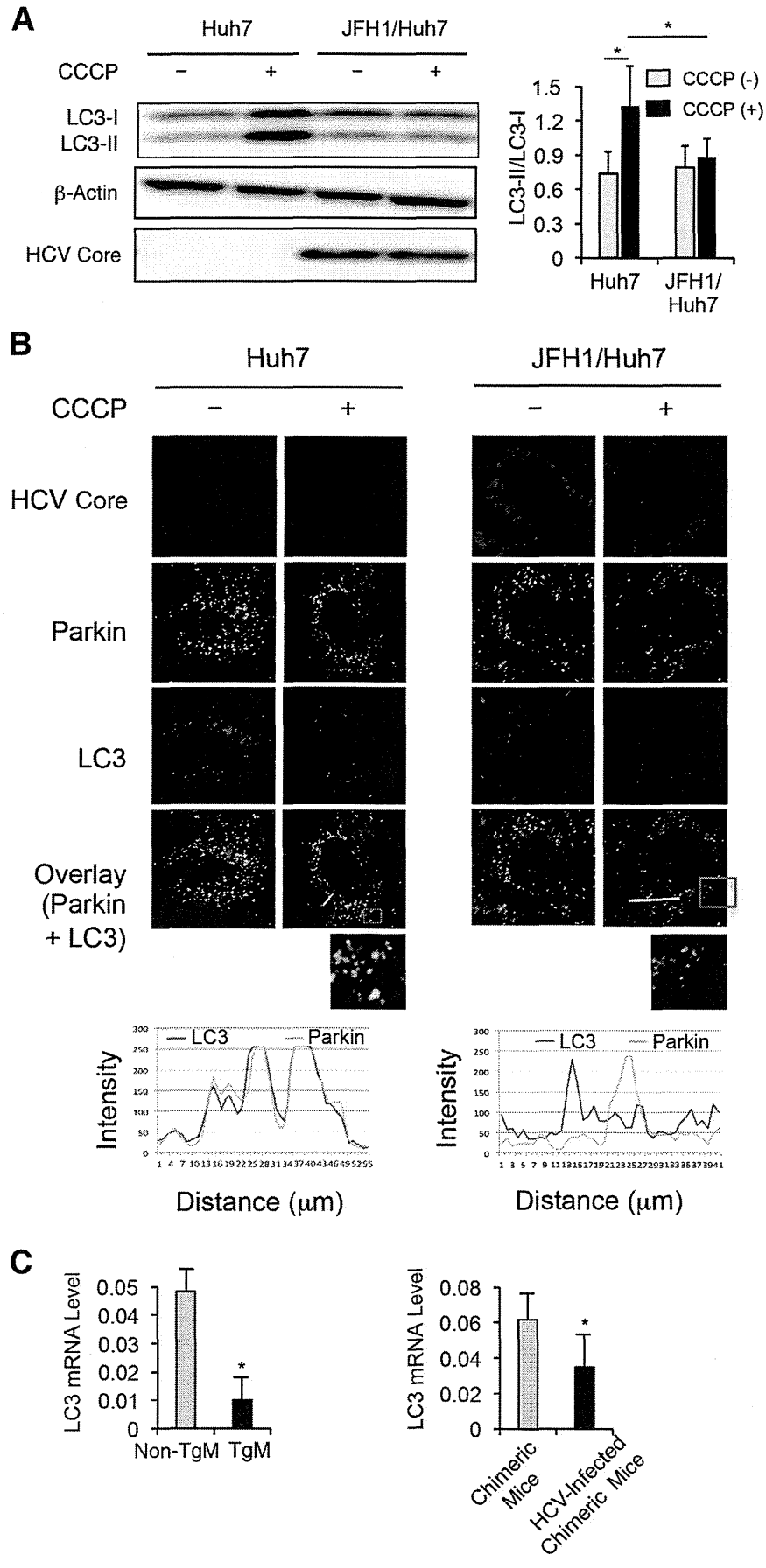

Figure 7 Effect of HCV infection on LC3-II expression and colocalization of Parkin with LC3 after carbonyl cyanide *m*-chlorophenylhydrazone (CCCP) treatment. **A:** Immunoblots for LC3-I and LC3-II using whole cell lysates of Huh7 and JFH1-Huh7 cells before and after CCCP treatment ($n = 5$). **B:** Immunofluorescence staining for Parkin (green) and LC3 (red) in Huh7 and JFH1-Huh7 cells before and after a 1-hour CCCP treatment. **Boxed areas** are enlarged below. Endogenous Parkin that colocalizes with LC3 (yellow spots). Line scans indicate the colocalization of Parkin with LC3 and correlate to the white lines in the images. **C:** The expression of LC3 mRNA in the liver from non-transgenic (non-TgM) and TgM mice ($n = 5$) and from chimeric mice without or with HCV infection ($n = 5$). The expression level of LC3 mRNA was normalized to GAPDH. $^*P < 0.05$.

mitochondria, was significantly reduced in JFH1-Huh7 cells compared with Huh7 cells (Figure 6F). Therefore, HCV infection clearly suppressed mitophagosome formation.

In agreement with suppressed mitophagosome formation, the LC3-II/I ratio was significantly lower after CCCP treatment in JFH1-Huh7 cells compared with Huh7 cells (Figure 7A), although the LC3-II/I ratio itself increased after CCCP treatment regardless of HCV infection. LC3 has been shown to be present in both complete autophagosomes and elongating isolation membranes that contain mitochondria ubiquitinated by Parkin. The present results indicate that Parkin colocalized with LC3 after CCCP treatment in Huh7 cells, whereas colocalization of Parkin and LC3 was significantly reduced in JFH1-Huh7 cells (Figure 7B). *In vivo*, FL-N/35-transgenic mice and HCV-infected chimeric mice also showed significantly reduced expression levels of LC3 mRNA in the liver compared with the control mice (Figure 7C), in agreement with reduced expression of Parkin in the mitochondrial fraction. These results may seem to be inconsistent with increased protein level of LC3-II after CCCP treatment *in vitro*. However, the lower LC3-II/I ratio after CCCP treatment in HCV-infected cells than in noninfected cells may reflect reduced expression levels of LC3 mRNA in FL-N/35-transgenic mice and HCV-infected chimeric mice. Further studies are required to clarify the mechanisms.

Several previous studies have proposed that autophagosome accumulation is enhanced on HCV infection and in HCV replicon cell lines.[34–38] Our findings of a decreased LC3-II/I ratio in JFH1-Huh7 cells, FL-N/35-transgenic mice, and HCV-infected chimeric mice seemingly contradict these previous reports. To clarify whether the decrease in LC3-II/I ratio observed in the present study indicated that macroautophagy (generally referred to as autophagy) or mitophagy was inhibited, we investigated LC3-II/I ratio in JFH1-Huh7 and Huh7 cells using Earle's balanced salt solution (EBSS) as a macroautophagy inducer (via amino acid starvation).[39] Interestingly, JFH1-Huh7 cells showed significantly increased LC3-II/I ratio compared with Huh7 cells after incubation with EBSS for 1 hour (Figure 8A), suggesting that HCV infection promoted autophagy under macroautophagy-inducible conditions. In agreement with increased LC3-II/I ratio, electron microscopy revealed that the number of autophagosomes was significantly greater after EBSS treatment in JFH1-Huh7 cells than in Huh7 cells (Figure 8B). Taken together with these results, the decrease in LC3-II/I ratio observed after CCCP treatment in JFH1-Huh7 cells likely represents a consequence of mitophagy inhibition, but not autophagy inhibition by HCV infection.

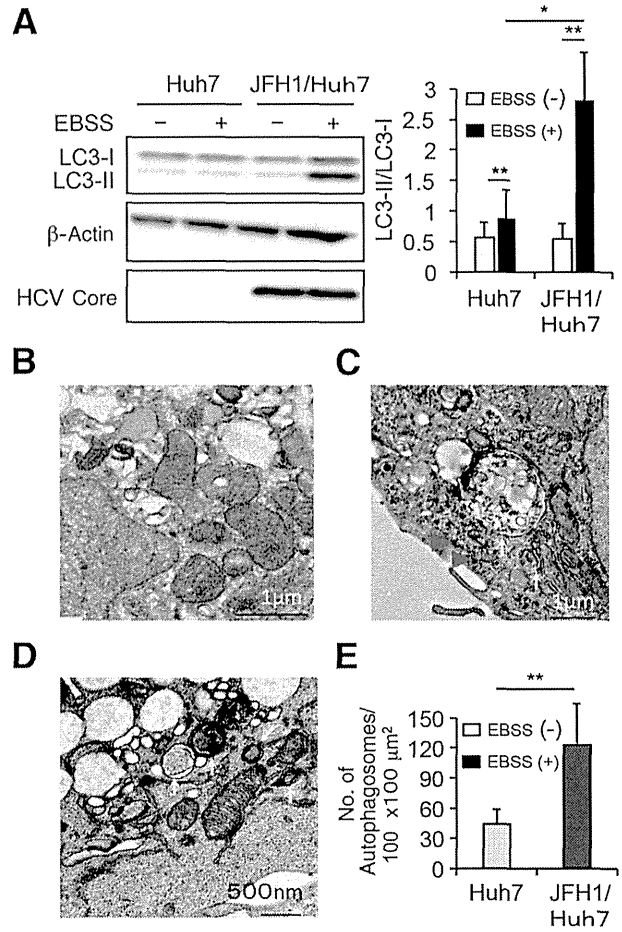

Figure 8 Effect of HCV infection on LC3-II expression and autophagosome formation after culture with Earle's balanced salt solution (EBSS). **A:** Immunoblots for LC3-II using Huh7 and JFH1-Huh7 cells before (−) and after (+) culture with EBSS ($n = 6$). The LC3-II and LC3-I expression level was normalized to β-actin. Electron microscopy of Huh7 (**B**) and JFH1-Huh7 (**C** and **D**) cells after EBSS treatment. The **arrows** indicate autophagosomes; **arrowheads,** HCV core protein. **E:** The number of autophagosomes per 100 × 100 μm² was calculated for five randomly selected views. $^{*}P < 0.05$, $^{**}P < 0.01$.

Suppression of Autophagic Degradation

The autophagic adaptor p62 can both aggregate ubiquitinated proteins by polymerizing with other p62 molecules and recruit ubiquitinated cargo into mitophagosomes by binding to LC3-II.[13] Therefore, p62 accumulation can be attributed to a deficit in autophagic degradation activity. After a 1- or 2-hour CCCP treatment, there was a smaller decrease in p62 in JFH1-Huh7 cells compared with Huh7 cells (Figure 9A). *In vivo*, FL-N/35-transgenic mice and HCV-infected chimeric mice also showed p62 accumulation in the liver compared with the control mice (Figure 9B). These results suggest that the degradation of damaged mitochondria was suppressed in the presence of HCV infection.

Finally, we assessed the change in VDAC1 content after CCCP treatment to obtain additional evidence as to whether mitophagy itself was suppressed by HCV infection. After a 2-hour CCCP treatment, a decrease in cellular content of VDAC1 was significantly smaller in JFH1-Huh7 cells than in Huh7 cells (Figure 9C). We also found that CCCP-induced increase in ROS production was greater in

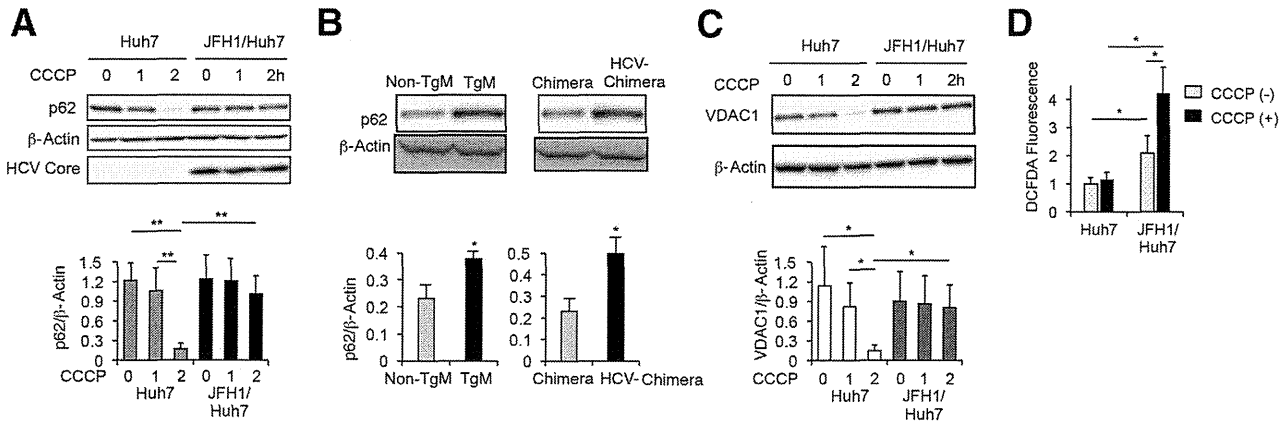

Figure 9 Effect of HCV infection on cellular p62 and VDAC1 expression after carbonyl cyanide *m*-chlorophenylhydrazone (CCCP) treatment and reactive oxygen species (ROS) production. **A:** Immunoblots for p62 using whole cell lysates of Huh7 and JFH1-Huh7 cells before and after a 1- and a 2-hour CCCP treatment ($n = 5$). **B:** Immunoblots for p62 using the liver from non-transgenic (non-TgM) and TgM ($n = 5$) mice and from chimeric mice without or with HCV infection ($n = 5$). The p62 expression level was normalized to β-actin. **C:** Immunoblots for VDAC1 using whole cell lysates of Huh7 and JFH1-Huh7 cells before and after a 1- and a 2-hour CCCP treatment ($n = 5$). The VDAC1 expression level was normalized to β-actin. **D:** Changes in cellular ROS production after a 1-hour CCCP treatment in Huh7 and JFH1-Huh7 cells ($n = 5$). $^*P < 0.05$, $^{**}P < 0.01$.

JFH1-Huh7 cells than in Huh7 cells (Figure 8D). These results were consistent with a previous study that showed an essential role of mitophagy in reducing mitochondrial ROS production[40] and, therefore, may reflect the suppressed mitophagy in the presence of HCV infection.

Discussion

Mitophagy may likely be induced in HCV-JFH1–infected cells in the context of mitochondrial depolarization, and in transgenic mice expressing the HCV polyprotein or in HCV-infected chimeric mice, both of which showed the decreased mitochondrial GSH content. Our results suggest that the HCV core protein inhibits mitophagy during HCV infection and that the molecular mechanisms by which this suppression occurs include the interaction of the HCV core protein with Parkin and the inhibition of Parkin translocation to the mitochondria. This inhibition leads to the failure of mitochondrial ubiquitination, mitophagosome formation, and autophagic degradation (Figure 10). Because Parkin 1 to 215 contains one of the critical amino acids required for mitochondrial localization, the specific interaction of Parkin 1 to 215 with the HCV core protein strongly suggests that the core protein represses mitophagy by inhibiting Parkin translocation to the mitochondria. We know that PINK1 accumulates in the mitochondria and phosphorylates Parkin after CCCP treatment and that the suppression of the mitochondrial Parkin signal occurs by blocking PINK1 via siRNA. Therefore, we could exclude the possibility that PINK1 plays a role in suppressing the recruitment of Parkin to the mitochondria. To our knowledge, this is the first report to demonstrate a suppressive effect of a viral protein on mitophagy via an interaction with Parkin. Interestingly, silencing Parkin via siRNA inhibited HCV core expression, which was consistent with the results of a recent study.[28] These results suggest that HCV potentially uses Parkin for its replication through the interaction between the HCV core protein and Parkin. Parkin may be post-transcriptionally involved in HCV replication, because Parkin silencing did not affect HCV core mRNA levels.

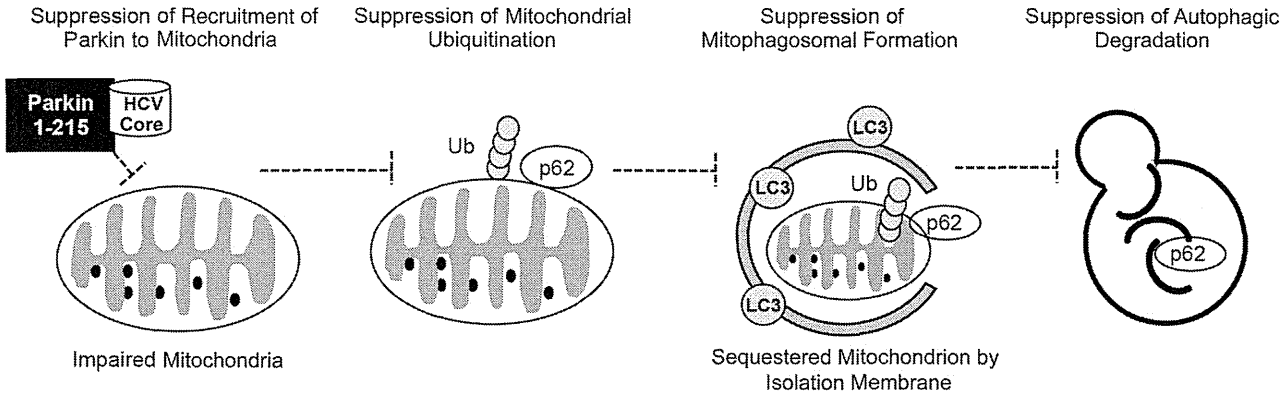

Figure 10 A schematic diagram depicting the mechanisms underlying mitophagy suppression by the HCV core protein. The HCV core protein interacts with the Parkin N-terminal fragment containing the RINGO domain (designated Parkin 1 to 215) and inhibits Parkin translocation to the mitochondria, which leads to the failure of mitochondrial ubiquitination, autophagosome formation, and autophagic degradation. Ub, ubiquitin.

Further studies are required to clarify the mechanisms underlying this speculation.

Two types of autophagy have been identified: nonselective and selective. For nonselective autophagy related to HCV infection, previous studies have reported the enhanced accumulation of autophagosomes without any effect on autophagic protein degradation,[33] the requirement of LC3 for efficient HCV replication,[34] and the occurrence of HCV RNA replication on autophagosomal membranes.[36] Mitophagy is selective and is induced by mitochondrial membrane depolarization, followed by Parkin recruitment to the mitochondria.[9–15] Herein, mitophagosome accumulation was suppressed because of mitophagy inhibition, whereas HCV infection enhanced the expression of LC3-II and autophagosome accumulation under nonselective autophagy-inducible conditions. Therefore, the present results are consistent with the previously characterized HCV-induced nonselective autophagic response.[34,35,38] However, a recent report has shown that HCV induces the mitochondrial translocation of Parkin and subsequent mitophagy,[28] which contrasts with the present results, except for the inhibitory effect of Parkin silencing on HCV replication. One of the significant differences in the method between the two studies was the presence or absence of CCCP treatment. Whether HCV-induced mitophagy was preceded by mitochondrial depolarization was unknown because $\Delta\Psi$ was not measured in the previous report of HCV-induced mitophagy.[28] However, we need to be careful that the mitochondrial depolarization by CCCP treatment is not a pathophysiological condition observed in HCV infection and that CCCP causes the depolarization of the entire mitochondrial network.[41] It is currently unknown whether CCCP treatment caused paradoxical results on mitophagy in HCV-infected cells between our study and a previous one.[28] Although suppressed mitophagy was also found in FL-N/35-transgenic mice and HCV-infected chimeric mice without any treatment, these mice may not be simply compared with HCV-JFH1–infected cells in terms of extremely low levels of viral proteins in FL-N/35-transgenic mice or spontaneous oxidized mitochondrial glutathione in both mice. Another difference between two studies was postinfection time from infection to assessment of mitophagy in HCV-JFH1–infected cells (21 versus 3 days). However, further studies are required to clarify whether postinfection time of HCV-JFH1–infected cells affects the interaction of HCV with Parkin. Oxidative stress and/or hepatocellular mitochondrial alterations are present in chronic hepatitis C to a greater degree than in other inflammatory liver diseases,[1,6] and mitophagy is important for maintaining mitochondrial quality by eliminating damaged mitochondria. Therefore, our results that the HCV core protein suppresses mitophagy appear reasonable in the context of what is known about the pathophysiological characteristics of chronic hepatitis C.

HCV-induced mitochondrial injury, ROS production, and subsequent oxidative stress contribute to HCC development in FL-N/35-transgenic mice that receive modest iron supplementation.[8] The relatively long period (12 months) required for HCC development suggests that mitochondrial injury, as a source of oxidative stress, must continue for a prolonged period. Mitochondrial DNA mutations are also relevant to HCC development in patients with chronic HCV infections.[42] Indeed, mitophagy plays an essential role in reducing mitochondrial ROS production and mitochondrial DNA mutations in yeast[40] and eliminating oxidative damaged mitochondria.[43] In addition to the directly induced generation of ROS by HCV proteins, the suppression of mitophagy by the HCV core protein has the potential to generate an additional long-lasting ROS burden and may offset or overwhelm the physiological antioxidative activity in mitochondria. Therefore, the suppressive effect of the HCV core protein on mitophagy may be an important mechanism of HCV-induced hepatocarcinogenesis.

In conclusion, results indicate that HCV core protein suppresses mitophagy by inhibiting Parkin translocation to the mitochondria via a direct interaction with Parkin in the context of mitochondrial depolarization. These findings have implications for the amplification and sustainability of mitochondria-induced oxidative stress observed in patients with HCV-related chronic liver disease and an increased risk of hepatocarcinogenesis.

Acknowledgments

We thank Dr. Stanley M. Lemon for the transgenic mice, Dr. Takaji Wakita for the JFH1 clone, and Hikari Hara for technical assistance.

References

1. Farinati F, Cardin R, De Maria N, Della Libera G, Marafin C, Lecis E, Burra P, Floreani A, Cecchetto A, Naccarato R: Iron storage, lipid peroxidation and glutathione turnover in chronic anti-HCV positive hepatitis. J Hepatol 1995, 22:449–456
2. Valgimigli M, Valgimigli L, Trere D, Gaiani S, Pedulli GF, Gramantieri L, Bolondi L: Oxidative stress EPR measurement in human liver by radical-probe technique: correlation with etiology, histology and cell proliferation. Free Radic Res 2002, 36:939–948
3. Okuda M, Li K, Beard MR, Showalter LA, Scholle F, Lemon SM, Weinman SA: Mitochondrial injury, oxidative stress, and antioxidant gene expression are induced by hepatitis C virus core protein. Gastroenterology 2002, 122:366–375
4. Moriya K, Nakagawa K, Santa T, Shintani Y, Fujie H, Miyoshi H, Tsutsumi T, Miyazawa T, Ishibashi K, Horie T, Imai K, Todoroki T, Kimura S, Koike K: Oxidative stress in the absence of inflammation in a mouse model for hepatitis C virus-associated hepatocarcinogenesis. Cancer Res 2001, 61:4365–4370
5. Korenaga M, Wang T, Li Y, Showalter LA, Chan T, Sun J, Weinman SA: Hepatitis C virus core protein inhibits mitochondrial electron transport and increases reactive oxygen species (ROS) production. J Biol Chem 2005, 280:37481–37488
6. Barbaro G, Di Lorenzo G, Asti A, Ribersani M, Belloni G, Grisorio B, Filice G, Barbarini G: Hepatocellular mitochondrial alterations in patients with chronic hepatitis C: ultrastructural and biochemical findings. Am J Gastroenterol 1999, 94:2198–2205

7. Nishina S, Hino K, Korenaga M, Vecchi C, Pietrangelo A, Mizukami Y, Furutani T, Sakai A, Okuda M, Hidaka I, Okita K, Sakaida I: Hepatitis C virus-induced reactive oxygen species raise hepatic iron level in mice by reducing hepcidin transcription. Gastroenterology 2008, 134:226–238
8. Furutani T, Hino K, Okuda M, Gondo T, Nishina S, Kitase A, Korenaga M, Xiao SY, Weinman SA, Lemon SM, Sakaida I, Okita K: Hepatic iron overload induces hepatocellular carcinoma in transgenic mice expressing the hepatitis C virus polyprotein. Gastroenterology 2006, 130:2087–2098
9. Kim I, Rodriguez-Enriquez S, Lemasters JJ: Selective degradation of mitochondria by mitophagy. Arch Biochem Biophys 2007, 462:245–253
10. Elmore SP, Qian T, Grissom S, Lemasters JJ: The mitochondrial permeability transition initiates autophagy in rat hepatocytes. FASEB J 2001, 15:2286–2287
11. Matsuda N, Sato S, Shiba K, Okatsu K, Saisho K, Gautier CA, Sou YS, Saiki S, Kawajiri S, Sato F, Kimura M, Komatsu M, Hattori N, Tanaka K: PINK1 stabilized by mitochondrial depolarization recruits Parkin to damaged mitochondria and activates latent Parkin for mitophagy. J Cell Biol 2010, 189:211–221
12. Narendra DP, Jin SM, Tanaka A, Suen DF, Gautier CA, Shen J, Cookson MR, Youle RJ: PINK1 is selectively stabilized on impaired mitochondria to activate Parkin. PLoS Biol 2010, 8:e1000298
13. Geisler S, Holmström KM, Skujat D, Fiesel FC, Rothfuss OC, Kahle PJ, Springer W: PINK1/Parkin-mediated mitophagy is dependent on VDAC1 and p62/SQSTM1. Nat Cell Biol 2010, 12:119–131
14. Vives-Bauza C, Zhou C, Huang Y, Cui M, de Vries RL, Kim J, May J, Tocilescu MA, Liu W, Ko HS, Magrane J, Moore DJ, Dawson VL, Grailhe R, Dawson TM, Li C, Tieu K, Przedborski S: PINK1-dependent recruitment of Parkin to mitochondria in mitophagy. Proc Natl Acad Sci USA 2010, 107:378–383
15. Narendra D, Tanaka A, Suen DF, Youle RJ: Parkin is recruited selectively to impaired mitochondria and promotes their autophagy. J Cell Biol 2008, 183:795–803
16. Chan NC, Salazar AM, Pham AH, Sweredoski MJ, Kolawa NJ, Graham RL, Hess S, Chan DC: Broad activation of the ubiquitin-proteasome system by Parkin is critical for mitophagy. Hum Mol Genet 2011, 20:1726–1737
17. Gegg ME, Cooper JM, Chau KY, Rojo M, Schapira AH, Taanman JW: Mitofusin 1 and mitofusin 2 are ubiquitinated in a PINK1/parkin-dependent manner upon induction of mitophagy. Hum Mol Genet 2010, 19:4861–4870
18. Chen D, Gao F, Li B, Wang H, Xu Y, Zhu C, Wang G: Parkin mono-ubiquitinates Bcl-2 and regulates autophagy. J Biol Chem 2010, 285: 38214–38223
19. Narendra D, Kane LA, Hauser DN, Fearnley IM, Youle RJ: p62/SQSTM1 is required for Parkin-induced mitochondrial clustering but not mitophagy: VDAC1 is dispensable for both. Autophagy 2010, 6:1090–1106
20. Itakura E, Kishi-Itakura C, Koyama-Honda I, Mizushima N: Structures containing Atg9A and the ULK1 complex independently target depolarized mitochondria at initial stages of Parkin-mediated mitophagy. J Cell Sci 2012, 125:1488–1499
21. Okatsu K, Saisho K, Shimanuki M, Nakada K, Shitara H, Sou YS, Kimura M, Sato S, Hattori N, Komatsu M, Tanaka K, Matsuda N: p62/SQSTM1 cooperates with Parkin for perinuclear clustering of depolarized mitochondria. Genes Cells 2010, 15:887–900
22. Wakita T, Pietschmann T, Kato T, Date T, Miyamoto M, Zhao Z, Murthy K, Habermann A, Kräusslich HG, Mizokami M, Bartenschlager R, Liang TJ: Production of infectious hepatitis C virus in tissue culture from a cloned viral genome. Nat Med 2005, 11:791–796
23. Li K, Prow T, Lemon SM, Beard MR: Cellular response to conditional expression of hepatitis C virus core protein in Huh7 cultured human hepatoma cells. Hepatology 2002, 35:1237–1246
24. Lerat H, Honda M, Beard MR, Loesch K, Sun J, Yang Y, Okuda M, Gosert R, Xiao SY, Weinman SA, Lemon SM: Steatosis and liver cancer in transgenic mice expressing the structural and nonstructural proteins of hepatitis C virus. Gastroenterology 2002, 122:352–365
25. Tateno C, Yoshizane Y, Saito N, Kataoka M, Utoh R, Yamasaki C, Tachibana A, Soeno Y, Asahina K, Hino H, Asahara T, Yokoi T, Furukawa T, Yoshizato K: Near completely humanized liver in mice shows human-type metabolic responses to drugs. Am J Pathol 2004, 165:901–912
26. Kimura T, Imamura M, Hiraga N, Hatakeyama T, Miki D, Noguchi C, Mori N, Tsuge M, Takahashi S, Fujimoto Y, Iwao E, Ochi H, Abe H, Maekawa T, Arataki K, Tateno C, Yoshizato K, Wakita T, Okamoto T, Matsuura Y, Chayama K: Establishment of an infectious genotype 1b hepatitis C virus clone in human hepatocyte chimeric mice. J Gen Virol 2008, 89:2108–2113
27. Ando M, Korenaga M, Hino K, Ikeda M, Kato N, Nishina S, Hidaka I, Sakaida I: Mitochondrial electron transport inhibition in full genomic hepatitis C replicon cells is restored by reducing viral replication. Liver Int 2008, 28:1158–1166
28. Kim SJ, Syed GH, Siddiqui A: Hepatitis C virus induces the mitochondrial translocation of Parkin and subsequent mitophagy. PLoS Pathog 2013, 9:e1003285
29. Toida K, Kosaka K, Aika Y, Kosaka T: Chemically defined neuron groups and their subpopulations in the glomerular layer of the rat main olfactory bulb. IV: intraglomerular synapses of tyrosine hydroxylase-immunoreactive neurons. Neuroscience 2000, 101:11–17
30. Ikeda M, Sugiyama K, Mizutani T, Tanaka T, Tanaka K, Sekihara H, Shimotohno K, Kato N: Human hepatocyte clonal cell lines that support persistent replication of hepatitis C virus. Virus Res 1998, 56: 157–167
31. Zhang GJ, Liu HW, Yang L, Zhong YG, Zheng YZ: Influence of membrane physical state on the lysosomal proton permeability. J Membr Biol 2000, 175:53–62
32. Sharpe MA, Wrigglesworth JM, Loewen J, Nicholls P: Small pH gradients inhibit cytochrome c oxidase: implications for H+ entry to the binuclear center. Biochem Biophys Res Commun 1995, 216: 931–938
33. Hristova VA, Beasley SA, Rylett RJ, Shaw GS: Identification of a novel Zn2+-binding domain in the autosomal recessive juvenile Parkinson-related E3 ligase parkin. J Biol Chem 2009, 284:14978–14986
34. Sir D, Chen WL, Choi J, Wakita T, Yen TS, Ou JH: Induction of incomplete autophagic response by hepatitis C virus via the unfolded protein response. Hepatology 2008, 48:1054–1061
35. Dreux M, Gastaminza P, Wieland SF, Chisari FV: The autophagy machinery is required to initiate hepatitis C virus replication. Proc Natl Acad Sci U S A 2009, 106:14046–14051
36. Ke PY, Chen SS: Activation of the unfolded protein response and autophagy after hepatitis C virus infection suppresses innate antiviral immunity in vitro. J Clin Invest 2011, 121:37–56
37. Sir D, Kuo CF, Tian Y, Liu HM, Huang EJ, Jung JU, Machida K, Ou JH: Replication of hepatitis C virus RNA on autophagosomal membranes. J Biol Chem 2012, 287:18036–18043
38. Shrivastava S, Bhanja Chowdhury J, Steele R, Ray R, Ray RB: Hepatitis C virus upregulates Beclin1 for induction of autophagy and activates mTOR signaling. J Virol 2012, 86:8705–8712
39. Munafo DB, Colombo MI: A novel assay to study autophagy: regulation of autophagosome vacuole size by amino acid deprivation. J Cell Sci 2001, 114:3619–3629
40. Kurihara Y, Kanki T, Aoki Y, Hirota Y, Saigusa T, Uchiumi T, Kang D: Mitophagy plays an essential role in reducing mitochondrial production of reactive oxygen species and mutation of mitochondrial DNA by maintaining mitochondrial quantity and quality in yeast. J Biol Chem 2012, 287:3265–3272
41. Wang Y, Nartiss Y, Steipe B, McQibban GA, Kim PK: ROS-induced mitochondrial depolarization initiates PARK2/PARKIN-dependent mitochondrial degradation by autophagy. Autophagy 2012, 8:1462–1476
42. Nishikawa M, Nishiguchi S, Shiomi S, Tamori A, Koh N, Takeda T, Kubo S, Hirohashi K, Kinoshita H, Sato E, Inoue M: Somatic mutation of mitochondrial DNA in cancerous and noncancerous liver tissue in individuals with hepatocellular carcinoma. Cancer Res 2001, 61:1843–1845
43. Venditti P, Di Stefano L, Di Meo S: Mitochondrial metabolism of reactive oxygen species. Mitochondrion 2013, 13:71–82

ANTICANCER RESEARCH *34*: 3125-3130 (2014)

Gemcitabine-based Adjuvant Chemotherapy for Patients with Advanced Gallbladder Cancer

MASAFUMI NAKAMURA[1], HIROSHI NAKASHIMA[1], TOSHIYA ABE[1], TAKAAKI ENSAKO[1], KOJI YOSHIDA[2] and KEISUKE HINO[2]

Departments of [1]Digestive Surgery and [2]Hepatology and Pancreatology, Kawasaki Medical School, Kurashiki, Japan

Abstract. *Aim: We investigated effects of gemcitabine-based adjuvant chemotherapy (GEM) on prognosis of patients with gallbladder cancer. Patients and Methods: We retrospectively analyzed outcomes of 36 patients who underwent radical resection for gallbladder cancer from 2001 through to 2012, using χ^2 for prognostic factors and Kaplan–Meier estimator and log-rank tests for survival data. Results: The GEM group had higher rates of lymph node positivity and distant metastasis, higher UICC stage and fewer R0 resections; their 5-year survival rate (60%) did not significantly differ from that of the controls (70.0%), nor was GEM a significant prognostic factor in univariate analysis. However, among patients who underwent R1 and R2 resections, GEM significantly improved prognosis in both univariate and multivariate analyses. Median survival of the R1/2 GEM group (66.4 months) was significantly better than that of controls (5.4 months) ($p=0.002$). Conclusion: GEM improved prognosis of patients with gallbladder cancer after R1/R2 resections.*

The efficacy of adjuvant chemotherapy for gallbladder cancer is currently unclear. Few studies have described the effect of adjuvant chemotherapy on biliary tract cancer (BTC) (1, 2), and only one phase III trial of adjuvant chemotherapy for BTC patients has been published. Clinical BTC research is limited by the small number of patients, and by the variety of cancers (bile duct, gallbladder and ampulla vater) which may differ in biological character (2). In this retrospective study, we focused exclusively on gallbladder cancer, and the therapeutic role of GEM in treating it.

Correspondence to: M. Nakamura, Department of Digestive Surgery, Kawasaki Medical School, 577 Matsushima, Kurashiki, 701-0192, Japan. Tel: +81 864621111, Fax: +81 864627897, e-mail: mnakamura@med.kawasaki-m.ac.jp

Key Words: Gallbladder cancer, curability, gemcitabine (GEM), adjuvant chemotherapy.

Patients and Methods

Patients. We retrospectively analyzed survival and characteristics of 36 patients who underwent radical resection for gallbladder cancer at the Kawasaki Medical School from 2001 to 2012. All patients gave their informed consent for surgical treatment. Out of these 36 patients, 7 underwent GEM with or without other drugs. Five of 7 patients underwent GEM monotherapy (six 28-day cycles: 1,000 mg/m^2/day gemcitabine on days 1, 8, and 15) (3). One of the 7 patients was treated with GEM and S-1 (each 21-day cycle: 1,000 mg/m^2/day gemcitabine on day 1 and 8; 60-100 mg/body oral S-1 according to body-surface area (<1.25 m^2, 60 mg/day; 1.25≤to<1.5 m^2, 80 mg/day; ≥1.5 m^2, 100 mg/d) on days 1 through 14)(4). Another of the 7 patient was treated with GEM and cisplatin (each 21-day cycle: cisplatin 25 mg/m^2 followed by gemcitabine 1,000 mg/m^2 on days 1 and 8) (5-7). 11 patients out of the 36 patients, 11 underwent R1 or R2 resections according to UICC definition (8). The mean follow-up period of this study was 29.7 months.

Statistical analysis. Statistical analysis and graphical presentations were performed with JMP 9 software (SAS Institute, Cary, NC, USA). Patients' characteristics were analyzed using the Mann–Whitney *U*-test and χ^2 test. Significance of prognostic factors was analyzed by χ^2 estimators of the proportional hazard model. Survival curves were constructed using the Kaplan–Meier product-limit method and were compared using the log-rank test. $p<0.05$ was considered statistically significant.

Results

Patients' characteristics. Patients treated with GEM (GEM group) showed higher UICC stage ($p<0.001$), higher rates of lymph node metastasis (N1, $p=0.004$), distant metastasis ($p=0.003$), peritoneal metastasis ($p=0.031$) and liver metastasis ($p=0.003$), and a lower rate of R0 resection ($p=0.009$), than patients who did not receive adjuvant chemotherapy (control group) (Table I) (8). Despite the advanced stage of disease in the GEM group, the two groups did not significantly differ in overall survival rate (OS), with 5-year survival rates of 60.0% for the GEM group and 70.0% for the control group ($p=0.566$; Table I and Figure 1).

0250-7005/2014 $2.00+.40

Table I. *Patients' characteristics.*

	All Patients	GEM group	Control group	*p*-Value
Total	36	7	29	
Gender (female)	17 (47.2%)	3 (42.9%)	14 (48.3%)	0.797
Age±SD (years)	75±8.0	70.0±2.9	76.1±1.4	0.070
Stage (0/IA/IB/IIA/IIB/III/IV)	6/2/13/3/8/0/4	0/0/0/0/4/0/3	6/2/13/3/4/0/1	>0.001*
T (0/is/1/2/3/4)	0/7/2/17/8/2	0/1/0/3/2/1	0/6/2/14/6/1	0.312
N1	10 (27.8%)	5 (71.4%)	5 (17.2%)	0.004*
Distant metastasis	4 (13.9%)	3 (42.9%)	1 (3.5%)	0.003*
Peritoneal	3 (8.3%)	2 (28.6%)	1 (3.5%)	0.031*
Liver	2 (5.6%)	2 (28.6%)	0 (0%)	0.003*
R0	23 9	2 (28.6%)	23 (79.3%)	0.009*
5-year survival rate	68.8%	60.0%	70.0%	0.566

GEM: Gemcitabine-based adjuvant chemotherapy. Staging, T, N1 and R0 were defined by classification of malignant tumors of UICC (6th ed.) (1). *$p<0.05$.

Univariate and multivariate analyses. We performed univariate and multivariate analyses of prognostic factors for 36 patients (Table II). Lower R0 resection rate, higher clinical stage, higher T-factor and positive lymph node metastasis (N1; as defined by UICC) were found to significantly predict worse prognosis by univariate analysis (8); out of these, higher T-factor and lymph-node metastasis were found to significantly predict worse prognosis by multivariate analysis (Table II). GEM was not a significant prognostic factor for the 36 patients (Table II).

Univariate and multivariate analyses of prognostic factors for patients who underwent R1 and R2 procedures. Univariate and multivariate analyses for patients with R1 and R2 procedures. In univariate analysis of prognostic factors for 11 patients who received R1 or R2 resections (Table II), lymph node metastasis and liver metastasis significantly predicted worse prognosis, and GEM predicted better prognosis (Table III). However, out of these 3 significant predictors in univariate analysis, only GEM remained significant in multivariate analysis (p=0.020; Table III). Accordingly, the GEM group's MST (66.4 months) was significantly better than the control group's MST (5.4 month) (p=0.002) (Figure 2).

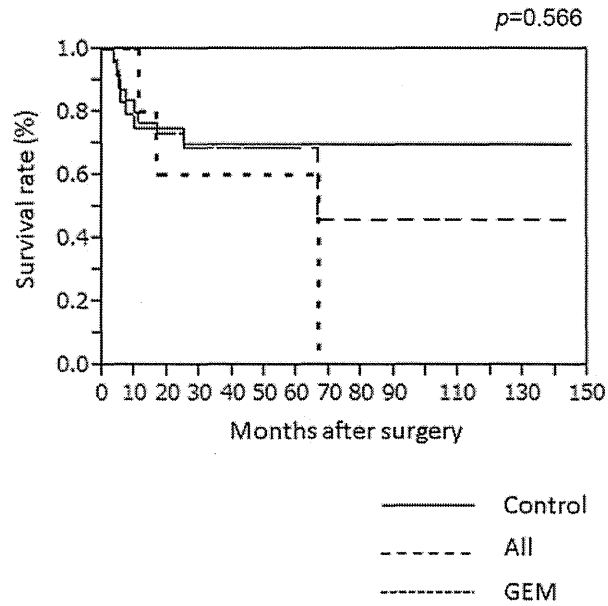

Figure 1. *Overall survival rate of patients with gallbladder cancer after radical surgery. Overall survival rates of all patients, those treated with gemcitabine-based adjuvant chemotherapy (GEM), and the control group were compared. p=0.566 for the GEM group vs the control group. p<0.05 was considered statistically significant.*

Discussion

We found that GEM was an independent significant prognostic factor for patients with gallbladder cancer with R1 or R2 curability (which itself predicts better prognosis).

The effects of adjuvant chemotherapy on BTC patients are not widely investigated (1); the aforementioned 2002 study from Takada *et al.* (9) is the only phase III randomized control trial to evaluate adjuvant chemotherapy for BTC patients. This study included not only BTC patients (118 with bile duct cancer, 112 with gallbladder cancer and 48 with ampullary cancer), but also 158 patients with pancreatic cancer. Survival of patients who were treated with MF therapy was compared against survival of patients treated with surgery-alone. The MF therapy improved prognosis of patients with gallbladder cancer (p=0.037), but not that of patients with pancreatic, bile duct, or ampullary cancers. Interestingly, the 5-year survival rates of patients who

Table II. *Univariate and multivariate analysis of prognostic factors.*

Factor	Univariate	Multivariate
Age	0.928	
Sex	0.105	
Stage	0.003*	0.246
T3,4	0.002*	0.022*
N1	0.001*	0.034*
Hepatectomy	0.706	
Resection of BD	0.102	
GEM	0.579	
Distant metastasis	0.198	
Liver	0.945	
Peritoneal	0.196	
R0	<0.001*	0.433

BD: Bile duct; GEM: gemcitabine-based adjuvant chemotherapy. Staging, T, N and R were defined by classification of malignant tumors of UICC (6th ed.) (12). *$p<0.05$.

Table III. *Univariate and multivariate analysis of prognostic factors for R1 and R2 patients.*

Factor	Univariate	Multivariate
Age	0.068	
Sex	0.412	
Stage	0.126	
T3,4	0.936	
N1	0.026*	0.138
Hepatectomy	0.234	
Resection of BD	0.615	
GEM	0.001*	0.020*
Distant metastasis	0.291	
Liver	0.020*	0.138
Peritoneal	0.742	

BD: Bile duct; GEM: gemcitabine-based adjuvant chemotherapy. Staging, T, N and R were defined by classification of malignant tumors of UICC (6th ed.) (12). *$p<0.05$.

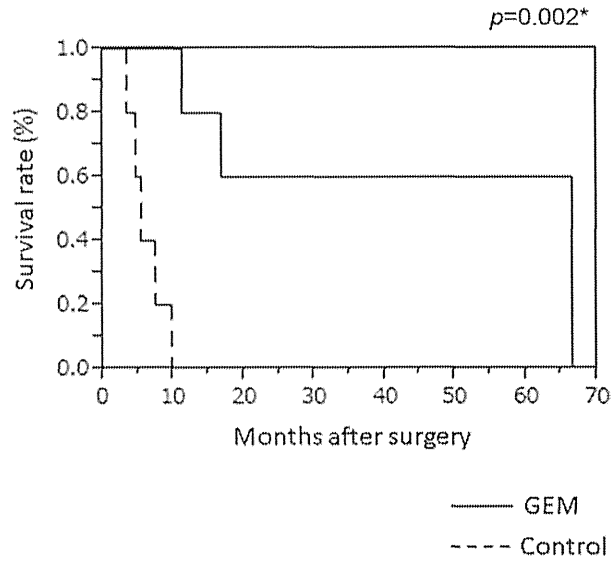

Figure 2. *Overall survival rate of patients with gallbladder cancer after R1 or R2 resections. Overall survival rates of patients treated with gemcitabine-based adjuvant chemotherapy (GEM) and the control group after R1 or R2 resection were compared. $p<0.05$ was considered statistically significant.*

underwent non-curative resections for gallbladder carcinomas was better in the MF group (8.9%) than in the control group (0%) (p=0.023); whereas among patients who underwent curative resections for gallbladder cancer, survival did not significantly differ between the two groups. As with the Takada study, GEM improved survival after R1 or R2 resection. We did not analyze patients who underwent R0 procedures because we had only 2 patients who received adjuvant chemotherapy after R0 resection.

Our results were also consistent with those of Murakami *et al.*, who retrospectively analyzed hilar bile duct cancer (10) in 42 patients, and found GEM to be a significant, single independent predictor of better prognosis (p=0.035) with 5-year survival rates of 57% and 23% for the GEM and control groups, respectively (p=0.026) (10). Another retrospective analysis from the Murakami group compared patients who received an adjuvant combination of gemcitabine and S-1 (GS) for UICC stage II BTC with patients without adjuvant chemotherapy (control group), and found GS-based adjuvant chemotherapy ($p<0.001$) and surgical margin status (p=0.003) were independent prognostic factors, with 5-year survival rates of 57% and 24% for GS and control groups, respectively ($p<0.001$) (11). However, prognosis of the GEM and control groups did not differ in our current study, possibly because the GEM group had more advanced gallbladder cancer than the control group in our study.

Recently, two groups reported on the effects of gemcitabine–cisplatin combination chemotherapy on unresectable BTC (2, 5-7). The National Cancer Research Network of UK organized the advanced BTC (ABC)-01 (phase II) and ABC-02 (phase III) studies (5, 6), which were both composed of two arms: one with gemcitabine–cisplatin combination chemotherapy, and one with gemcitabine monotherapy. Patients treated with combination therapy had significantly longer mean survival time (11.7 months) than those treated with gemcitabine-alone (8.3 months) ($p<0.001$) (6). The ABC study was confirmed by the BT22 trial in Japan (7), which showed median survival time for the combination arm (11.2 months) to be significantly longer than the monotherapy arm (7.7 months) (p=0.139) (7). In the present study, survival of R1 and R2 patients was improved

although we mainly used gemcitabine monotherapy as adjuvant chemotherapy. The BT22 and ABC studies suggest that we might further improve survival of patients with patients with gallbladder cancer by using a combination of cisplatin and gemcitabine as adjuvant therapy.

Effects of adjuvant radiotherapy are also controversial. Although 3 retrospective studies have reported that adjuvant radiotherapy improved prognosis of patients with microscopically-positive margins (12-14), Pitt *et al.* organized a prospective study showing that adjuvant radiotherapy did not improve survival of patients with hilar bile duct cancer (15).

The effects of adjuvant chemo-radiotherapy on BTC are also debated. Hughes *et al.* and Lim *et al.* showed significantly improved OS from adjuvant chemo-radiotherapy, whereas Nakeeb *et al.*, Krishnan *et al.* and Zhou *et al.* did not find a difference (16-20), and Gold *et al.* and Kim *et al.* found a limited effect (21, 22). Clinical research on BTC is complicated by the relatively few patients and the variety of origins, bile duct, gall bladder and ampulla vater. A prospective multi-Institutional joint investigation could overcome these difficulties.

This report is the first to focus exclusively on GEM adjuvant therapy in gallbladder cancer. Wider use of gemcitabine-based adjuvant chemotherapy could improve survival of patients with advanced gallbladder cancer, who currently have poor prognoses. A well-designed randomized prospective multi-Institutional joint investigation is warranted to improve the prognosis of these patients.

Conflicts of Interest

The Authors declare no conflicts of interest.

References

1 Uesaka K: Adjuvant therapy for resected biliary tract cancer. JJBA *24*: 689-694, 2010.

2 Furuse J, Okusaka T, Bridgewater J, Taketsuna M, Wasan H, Koshiji M and Valle J: Lessons from the comparison of two randomized clinical trials using gemcitabine and cisplatin for advanced biliary tract cancer. Crit Rev Oncol Hematol *80(1)*: 31-39, 2011.

3 Nakamura M, Kayashima T, Fujiwara K, Nagayoshi Y, Kono H, Ohtsuka T, Takahata S, Mizumoto K and Tanaka M: Combination therapy of portal vein resection and adjuvant gemcitabine improved prognosis of advanced pancreatic cancer. Hepatogastroenterology *60*: 354-357, 2013.

4 Ueno H, Ioka T, Ikeda M, Ohkawa S, Yanagimoto H, Boku N, Fukutomi A, Sugimori K, Baba H, Yamao K, Shimamura T, Sho M, Kitano M, Cheng AL, Mizumoto K, Chen JS, Furuse J, Funakoshi A, Hatori T, Yamaguchi T, Egawa S, Sato A, Ohashi Y, Okusaka T and Tanaka M: Randomized phase III study of gemcitabine plus S-1, S-1 alone, or gemcitabine alone in patients with locally advanced and metastatic pancreatic cancer in Japan and Taiwan: GEST study. J Clin Oncol *31*: 1640-1648, 2013.

5 Valle JW, Wasan H, Johnson P, Jones E, Dixon L, Swindell R, Baka S, Maraveyas A, Corrie P, Falk S, Gollins S, Lofts F, Evans L, Meyer T, Anthoney A, Iveson T, Highley M, Osborne R and Bridgewater J: Gemcitabine alone or in combination with cisplatin in patients with advanced or metastatic cholangiocarcinomas or other biliary tract tumours: a multicentre randomised phase II study - The UK ABC-01 Study. Br J Cancer *101*: 621-627, 2009.

6 Valle J, Wasan H, Palmer DH, Cunningham D, Anthoney A, Maraveyas A, Madhusudan S, Iveson T, Hughes S, Pereira SP, Roughton M and Bridgewater J: Cisplatin plus gemcitabine versus gemcitabine for biliary tract cancer. N Engl J Med *362*: 1273-1281, 2010.

7 Okusaka T, Nakachi K, Fukutomi A, Mizuno N, Ohkawa S, Funakoshi A, Nagino M, Kondo S, Nagaoka S, Funai J, Koshiji M, Nambu Y, Furuse J, Miyazaki M and Nimura Y: Gemcitabine alone or in combination with cisplatin in patients with biliary tract cancer: a comparative multicentre study in Japan. Br J Cancer *103*: 469-474, 2010.

8 Sobin LH, Gospodarowicz MK and Wittekind C: TNM Classification of Malignant Tumours Sixth Edition: Wiley-Liss; 2002.

9 Takada T, Amano H, Yasuda H, Nimura Y, Matsushiro T, Kato H, Nagakawa T and Nakayama T: Is postoperative adjuvant chemotherapy useful for gallbladder carcinoma? A phase III multicenter prospective randomized controlled trial in patients with resected pancreaticobiliary carcinoma. Cancer *95*: 1685-1695, 2002.

10 Murakami Y, Uemura K, Sudo T, Hayashidani Y, Hashimoto Y, Nakamura H, Nakashima A and Sueda T: Gemcitabine-based adjuvant chemotherapy improves survival after aggressive surgery for hilar cholangiocarcinoma. J Gastrointest Surg *13*: 1470-1479, 2009.

11 Murakami Y, Uemura K, Sudo T, Hayashidani Y, Hashimoto Y, Nakamura H, Nakashima A and Sueda T: Adjuvant gemcitabine plus S-1 chemotherapy improves survival after aggressive surgical resection for advanced biliary carcinoma. Ann Surg *250*: 950-956, 2009.

12 Todoroki T, Ohara K, Kawamoto T, Koike N, Yoshida S, Kashiwagi H, Otsuka M and Fukao K: Benefits of adjuvant radiotherapy after radical resection of locally advanced main hepatic duct carcinoma. Int J Radiat Oncol Biol Phys *46*: 581-587, 2000.

13 Schoenthaler R, Phillips TL, Castro J, Efird JT, Better A and Way LW: Carcinoma of the extrahepatic bile ducts. The University of California at San Francisco experience. Ann Surg *219*: 267-274, 1994.

14 Cheng Q, Luo X, Zhang B, Jiang X, Yi B and Wu M: Predictive factors for prognosis of hilar cholangiocarcinoma: postresection radiotherapy improves survival. Eur J Surg Oncol *33*: 202-207, 2007.

15 Pitt HA, Nakeeb A, Abrams RA, Coleman J, Piantadosi S, Yeo CJ, Lillemore KD and Cameron JL: Perihilar cholangiocarcinoma. Postoperative radiotherapy does not improve survival. Ann Surg *221*: 788-797; discussion 97-98, 1995.

16 Hughes MA, Frassica DA, Yeo CJ, Riall TS, Lillemoe KD, Cameron JL, Donehower RC, Laheru DA, Hruban RH and Abrams RA: Adjuvant concurrent chemoradiation for adenocarcinoma of the distal common bile duct. Int J Radiat Oncol Biol Phys *68*: 178-182, 2007.

17 Lim KH, Oh DY, Chie EK, Jang JY, Im SA, Kim TY, Kim SW, Ha SW and Bang YJ: Adjuvant concurrent chemoradiation therapy (CCRT) alone versus CCRT followed by adjuvant chemotherapy: which is better in patients with radically resected extrahepatic biliary tract cancer?: a non-randomized, single center study. BMC Cancer *9*: 345, 2009.
18 Nakeeb A, Tran KQ, Black MJ, Erickson BA, Ritch PS, Quebbeman EJ, Wilson SD, Demeure MJ, Rilling WS, Dua KS and Pitt HA: Improved survival in resected biliary malignancies. Surgery *132*: 555-563; discission 63-64, 2002.
19 Krishnan S, Rana V, Evans DB, Varadhachary G, Das P, Bhatia S, Delclos ME, Janjan NA, Wolff RA, Crane CH and Pisters PW: Role of adjuvant chemoradiation therapy in adenocarcinomas of the ampulla of vater. Int J Radiat Oncol Biol Phys *70*: 735-743, 2008.
20 Zhou J, Hsu CC, Winter JM, Pawlik TM, Laheru D, Hughes MA, Donehower R, Wolfgang C, Akbar U, Schulick R, Cameron J and Herman JM: Adjuvant chemoradiation versus surgery alone for adenocarcinoma of the ampulla of Vater. Radiother Oncol *92*: 244-248, 2009.
21 Gold DG, Miller RC, Haddock MG, Gunderson LL, Quevedo F, Donohue JH, Bhatia S and Nagorney DM: Adjuvant therapy for gallbladder carcinoma: the Mayo Clinic Experience. Int J Radiat Oncol Biol Phys *75*: 150-155, 2009.
22 Kim K, Chie EK, Jang JY, Kim SW, Oh DY, Im SA, Kim TY, Bang YJ and Ha SW: Role of adjuvant chemoradiotherapy for ampulla of Vater cancer. Int J Radiat Oncol Biol Phys *75*: 436-441, 2009.

Received February 24, 2014
Revised April 22, 2014
Accepted April 23, 2014

Hepatology Research

Hepatology Research 2014; 44: E229–E239 doi: 10.1111/hepr.12254

Original Article

Hepatic oxidative stress in ovariectomized transgenic mice expressing the hepatitis C virus polyprotein is augmented through suppression of adenosine monophosphate-activated protein kinase/proliferator-activated receptor gamma co-activator 1 alpha signaling

Yasuyuki Tomiyama, Sohji Nishina, Yuichi Hara, Tomoya Kawase and Keisuke Hino

Department of Hepatology and Pancreatology, Kawasaki Medical School, Kurashiki, Japan

Aim: Oxidative stress plays an important role in hepatocarcinogenesis of hepatitis C virus (HCV)-related chronic liver diseases. Despite the evidence of an increased proportion of females among elderly patients with HCV-related hepatocellular carcinoma (HCC), it remains unknown whether HCV augments hepatic oxidative stress in postmenopausal women. The aim of this study was to determine whether oxidative stress was augmented in ovariectomized (OVX) transgenic mice expressing the HCV polyprotein and to investigate its underlying mechanisms.

Methods: OVX and sham-operated female transgenic mice expressing the HCV polyprotein and non-transgenic littermates were assessed for the production of reactive oxygen species (ROS), expression of inflammatory cytokines and antioxidant potential in the liver.

Results: Compared with OVX non-transgenic mice, OVX transgenic mice showed marked hepatic steatosis and ROS production without increased induction of inflammatory cytokines, but there was no increase in ROS-detoxifying enzymes such as superoxide dismutase 2 and glutathione peroxidase 1. In accordance with these results, OVX transgenic mice showed less activation of peroxisome proliferator-activated receptor-γ co-activator-1α (PGC-1α), which is required for the induction of ROS-detoxifying enzymes, and no activation of adenosine monophosphate-activated protein kinase-α (AMPKα), which regulates the activity of PGC-1α.

Conclusion: Our study demonstrated that hepatic oxidative stress was augmented in OVX transgenic mice expressing the HCV polyprotein by attenuation of antioxidant potential through inhibition of AMPK/PGC-1α signaling. These results may account in part for the mechanisms by which HCV-infected women are at high risk for HCC development when some period has passed after menopause.

Key words: antioxidant potential, glutathione peroxidase, reactive oxygen species, superoxide dismutase

INTRODUCTION

PERSISTENT HEPATITIS C virus (HCV) infection is a major risk factor for the development of hepatocellular carcinoma (HCC) in Japan. Approximately 70% of Japanese HCC patients are currently diagnosed with HCV-associated cirrhosis or chronic hepatitis C.[1] Nevertheless, the mechanisms underlying HCV-associated hepatocarcinogenesis are incompletely understood. Notably, there is sex disparity in HCC development, that is, male sex has been demonstrated to be an independent risk factor associated with HCC development.[2–4] It is proposed that estrogen-mediated inhibition of interleukin (IL)-6 production by Kupffer cells reduces the HCC risk in females.[5] In addition, the proportion of females among elderly patients with HCV-related HCC has recently increased in Japan.[6] These results suggest that menopause may be a risk factor associated with HCC development in female patients with HCV infection.

Numerous studies have shown that oxidative stress is present in chronic hepatitis C to a greater degree than in other inflammatory disease,[7,8] and is related to

Correspondence: Professor Keisuke Hino, Department of Hepatology and Pancreatology, Kawasaki Medical School, 577 Matsushima, Kurashiki, Okayama 701-0192, Japan. Email: khino@med.kawasaki-m.ac.jp

Received 9 September 2013; revision 24 September 2013; accepted 30 September 2013.

hepatocarcinogenesis in HCV-associated chronic liver diseases.[9,10] We have previously demonstrated that transgenic mice expressing the HCV polyprotein develop liver tumors including HCC, in connection with oxidative stress induced by HCV and iron overload.[11] Interestingly, such hepatocarcinogenesis was observed only in male transgenic mice, suggesting that females are resistant to oxidative stress in these transgenic mice. On the other hand, it is reported that ovariectomy increases nicotinamide adenine dinucleotide phosphate (NADPH) oxidase activity[12] and decreases mitochondrial-reduced glutathione levels in rats.[13] However, it remains unknown how HCV affects ovariectomy-induced oxidative stress. Investigation of this issue may provide a clue for understanding why the incidence of HCC increases in elderly postmenopausal women with HCV infection. The aim of this study was to determine whether HCV proteins amplify oxidative stress induced by ovariectomy and to investigate the mechanisms underlying this.

METHODS

Animals

CONTAINING THE FULL-LENGTH polyprotein-coding region under the control of the murine albumin promoter/enhancer, the transgene pAlbSVPA-HCV has been described in detail.[14,15] Of the four transgenic lineages with evidence of RNA transcription of the full-length HCV-N open reading frame (FL-N), the FL-N/35 lineage proved capable of breeding in large numbers. There is no inflammation in the transgenic liver.[15]

Experimental design

Female FL-N/35 transgenic mice and their normal female C57BL/6 littermates were anesthetized for surgery and underwent either a bilateral ovariectomy or sham operation at the age of 4–6 weeks. We studied ovariectomized (OVX) transgenic mice ($n = 5$), sham-operated transgenic mice ($n = 5$), OVX non-transgenic mice ($n = 5$) and sham-operated non-transgenic mice ($n = 5$). These mice were fed a normal rodent diet, bred, maintained, and killed by i.p. injection of 10% pentobarbital sodium preceded by 20-h fasting at the age of 24 weeks. All experimental protocols and animal maintenance procedures used in this study were approved by the Ethics Review Committee for Animal Experimentation of Kawasaki Medical School.

Histological procedures

A portion of liver tissue was immediately snap-frozen in liquid nitrogen for determination of the hepatic triglyceride concentration. The remaining liver tissue was fixed in 4% paraformaldehyde in phosphate-buffered saline and embedded in paraffin for histological analyses. Liver sections were stained with hematoxylin–eosin.

Serum leptin concentration

The serum leptin level was measured using a Rat Leptin Elisa kit (Morinaga Institute of Biological Science, Yokohama, Japan) according to the manufacturer's instructions.

Hepatic triglyceride content

Lipids were extracted from the homogenized liver tissue by the method of Bligh and Dyer.[16] The triglyceride level was measured with a TGE-test Wako kit (Wako Pure Chemicals, Tokyo, Japan), according to the manufacturer's instructions. Protein concentrations in liver were determined by the method of Lowry *et al.*,[17] using a DC protein assay kit (Bio-Rad Laboratories, Hercules, CA, USA).

In situ detection of reactive oxygen species (ROS)

In situ ROS production in the liver was assessed by staining with dihydroethidium, as described previously.[18] In the presence of ROS, dihydroethidium (Invitrogen, Carlsbad, CA, USA) is oxidized to ethidium bromide and stains nuclei bright red by intercalating with the DNA.[19] Fluorescence intensity was quantified using National Institutes of Health image analysis software for 3 randomly selected areas of digital images for each mouse.

Hepatic iron content

Hepatic iron content was measured by atomic absorption spectrometry, as described previously,[11] and expressed as micrograms Fe per gram of tissue (wet weight).

Derivatives of reactive oxygen metabolites (dROM) and biological antioxidant potential (BAP)

The levels of dROM and BAP were measured using a Free Radical Elective Evaluator (Wismerll, Tokyo, Japan), as described previously.[20] Measurement of dROM is based on the ability of the transition metal ions to catalyze the formation of alkoxy and peroxy radicals from hydroper-

oxides present in serum. The results are expressed in conventional units as Carrtelli units (U.CARR), where 1 U.CARR corresponds to 0.8 mg/L H_2O_2. Measurement of BAP is based on the ability of antioxidants to reduce ferric (F^{3+}) ions to ferrous (Fe^{2+}) ions.

RNA isolation and real-time reverse transcription polymerase chain reaction (RT–PCR)

Total RNA was isolated using an RNeasy mini kit (QIAGEN, Hilden, Germany) and reverse-transcribed into cDNA by using a Superscript III reverse transcription kit (Invitrogen). The PCR reactions were run in the ABI Prism 7700 sequence detection system (Applied Biosystems, Foster, CA, USA). The levels of mRNA were determined using cataloged primers (Applied Biosystems) for mice (tumor necrosis factor [TNF]-α, Mm00443258_m1; IL-1β, Mm00434228_m1; IL-6, Mm00446190_m1; HAMP [gene encoding hepcidin], Mm00519025_mL; superoxide dismutase 2 [SOD2], Mm01313000_m1; glutathione peroxidase 1 [GPx1], Mm00656767_g1; and sirtuin 3 [SIRT3], Mm00452131_m1). Expression of these genes was normalized to expression of glyceraldehyde 3-phosphate dehydrogenase mRNA (GAPDH, Mm99999915_g1).

Isolation of mitochondria and nuclear fraction

Mitochondrial extraction from liver tissue was performed using a Qproteome Mitochondrial Isolation kit (QIAGEN) according to the manufacturer's instructions. The nuclear fraction from liver tissue was prepared using a Nuclear Extraction kit (Panomics, Fremont, CA, USA) according to the manufacturer's instructions.

Immunoblotting

Liver lysates and the mitochondrial and nuclear fractions from liver were separated by sodium dodecylsulfate polyacrylamide gel electrophoresis. The proteins were transferred to polyvinylidene difluoride membranes (Millipore, Bradford, MA, USA), blocked overnight at 4°C with 5% skim milk and 0.1% Tween-20 in Tris-buffered saline, and subsequently incubated for 1 h at room temperature with goat antihuman SOD2 antibody (Santa Cruz Biotechnology, Santa Cruz, CA, USA), rabbit antihuman GPx1 antibody (Abcam, Cambridge, MA, USA), rabbit antihuman SIRT3 antibody (Abcam), rabbit antihuman peroxisome proliferator-activated receptor-γ co-activator-1α (PGC-1α) antibody (Abcam), rabbit antihuman adenosine monophosphate-activated protein kinase-α (AMPKα) antibody (Cell Signaling Technology, Boston, MA, USA), rabbit antihuman phospho-AMPKα (Thr172) antibody (Cell Signaling Technology), rabbit antihuman mitochondrial heat shock protein 70 antibody (HSP70; Thermo Scientific, Rockford, IL, USA), rabbit antihuman β-actin antibody (Cell Signaling Technology) or rabbit antimouse lamin B1 antibody (Abcam). The membranes were washed and incubated with horseradish peroxidase (HRP)-conjugated donkey antigoat immunoglobulin (Ig)G (Santa Cruz Biotechnology) or HRP-conjugated donkey antirabbit IgG (GE Healthcare Life Sciences, Pittsburgh, PA, USA).

Statistical analysis

Quantitative values are expressed as mean ± standard deviation. Two groups among multiple groups were compared by the rank-based Kruskal–Wallis ANOVA test followed by Scheffé's test. The statistical significance of correlation was determined by the use of simple regression analysis. $P < 0.05$ was considered to be significant.

RESULTS

Ovariectomy enhanced hepatic steatosis in FL-N/35 transgenic mice

AS CONFIRMATION OF successful ovariectomy-induced suppression of endogenous estrogen production, the uterine weight of OVX mice was significantly decreased compared with that of sham-operated mice (Table 1). Dietary intake, bodyweight, liver weight and serum leptin levels were significantly greater in OVX mice than in sham-operated mice regardless of whether they were transgenic or non-transgenic (Table 1). Interestingly, the serum alanine aminotransferase (ALT) level was significantly higher in OVX transgenic mice than in mice in the other three groups, but the levels were comparable in OVX non-transgenic and sham-operated non-transgenic mice (Table 1). To determine why OVX transgenic mice have a higher ALT level, we investigated the liver histology of the mice in the four groups (OVX transgenic, sham-operated transgenic, OVX non-transgenic and sham-operated non-transgenic mice). In contrast to the mild to moderate degree of hepatic steatosis noted in OVX non-transgenic mice and sham-operated transgenic mice, OVX transgenic mice developed severe hepatic steatosis (Fig. 1a) without infiltration of inflammatory mononuclear cells. Hepatic triglyceride content was measured to quantify the degree of steatosis. The triglyceride content was significantly greater in OVX transgenic mice than in mice in the other three groups (Fig. 1b), which was consistent with the

Table 1 Body, liver and uterus weight and serum biochemical parameters

Body, liver, and uterus weight and serum biochemical parameters	Non-transgenic		Transgenic	
	Sham-operated	OVX	Sham-operated	OVX
Bodyweight (g)	21.5 ± 1.2	30.7 ± 4.9*	27.7 ± 4.6	34.2 ± 3.8**
Liver weight (g)	0.86 ± 0.075	1.09 ± 0.236*	0.90 ± 0.102	1.18 ± 0.156**
Ratio of liver to bodyweight	0.038 ± 0.037	0.035 ± 0.003	0.031 ± 0.002	0.034 ± 0.006
Uterus weight (g)	0.08 ± 0.01	0.01 ± 0.02*	0.09 ± 0.01	0.01 ± 0.01**
Total dietary intake (g)	337 ± 24	429 ± 13*	368 ± 28	490 ± 31**
Serum glucose (mg/dL)	222.9 ± 110.0	275.1 ± 121.4	284.0 ± 84.1	259.7 ± 108.9
Serum ALT (IU/L)	15.5 ± 6.5	30.6 ± 38.1	21.8 ± 11.4	281.2 ± 165.1***
Serum triglyceride (mg/dL)	99.9 ± 9.7	78.9 ± 10.8	98.3 ± 11.4	89.7 ± 13.3
Serum leptin (ng/mL)	0.45 ± 0.14	1.31 ± 0.31*	0.65 ± 0.22	1.60 ± 0.28**

Data are mean ± standard deviation.
*$P < 0.05$ compared with sham-operated non-transgenic mice. **$P < 0.05$ compared with sham-operated transgenic mice. ***$P < 0.01$ compared with mice in the other three groups.
ALT, alanine aminotransferase; OVX, ovariectomized.

results for hepatic steatosis. Thus, the increase in the serum ALT level in the OVX transgenic mice was thought to reflect the hepatic steatosis.

Ovariectomy increased ROS and IL-6 production in the liver

Only OVX transgenic mice showed marked hepatic steatosis, regardless of the comparable diet intake and the ratio of liver to bodyweight of OVX non-transgenic mice (Table 1). We have previously demonstrated that iron-overloaded male FL-N/35 transgenic mice expressing the HCV polyprotein develop severe hepatic steatosis through increased ROS production.[11] Therefore, we examined whether ROS production was relevant to the marked hepatic steatosis observed in the OVX transgenic mice. Ovariectomy significantly increased ROS (super-

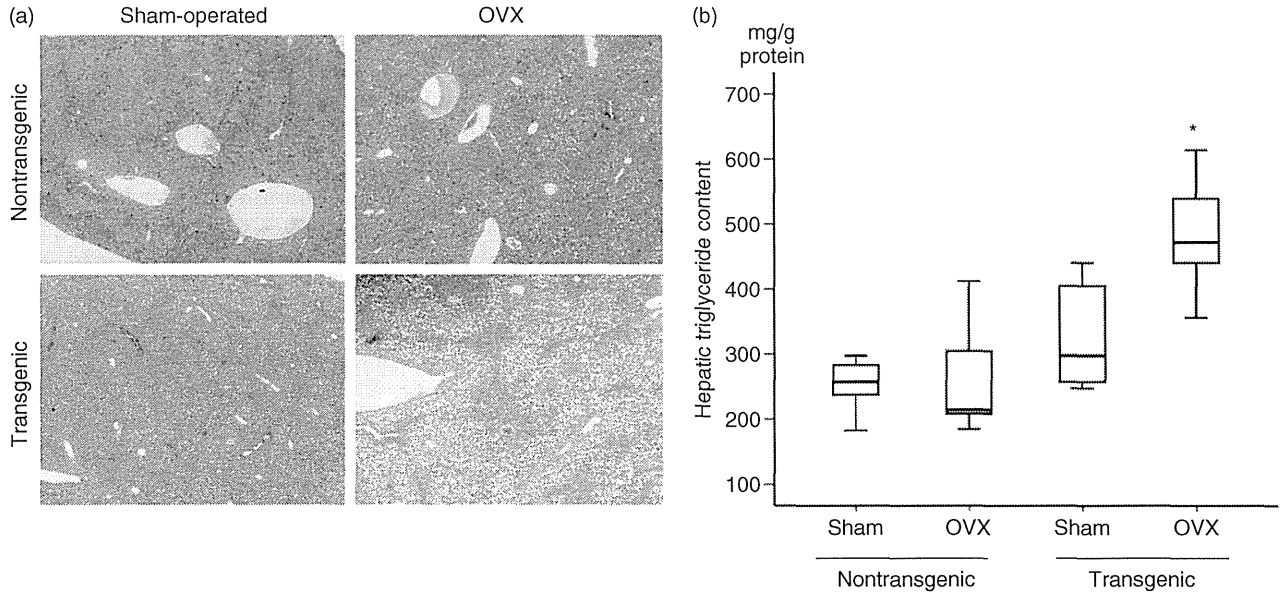

Figure 1 Hepatic steatosis and triglyceride content in sham-operated and ovariectomized (OVX) FL-N/35 transgenic and non-transgenic mice. (a) Hepatic steatosis in mice in each group (H&E, original magnification × 100). (b) Hepatic triglyceride content in mice in each group ($n = 5$). The results are shown as box plot profiles. The bottom and top edges of the boxes are the 25th and 75th percentiles, respectively. Median values are shown by the line within each box. *: $P < 0.05$ versus mice in the other three groups.

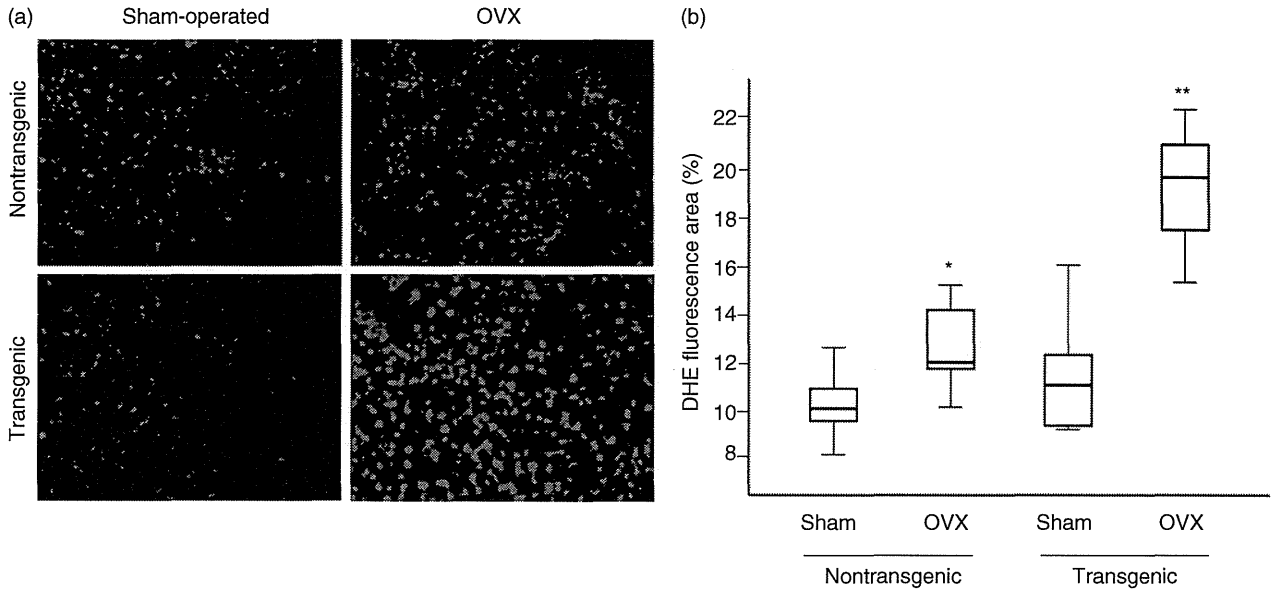

Figure 2 Reactive oxygen species (ROS) production in sham-operated and ovariectomized (OVX) FL-N/35 transgenic and non-transgenic mice. (a) Frozen liver sections from mice in each group were stained with dihydroethidium (DHE). (b) Fluorescence intensity was quantified by NIH image analysis software for three randomly selected areas of digital images for five mice in each group. The results are shown as box plot profiles. The bottom and top edges of the boxes are the 25th and 75th percentiles, respectively. Median values are shown by the line within each box. *: $P < 0.05$ versus sham-operated non-transgenic mice. **: $P < 0.05$ versus sham-operated nontransgenic mice, OVX non-transgenic mice and sham-operated transgenic mice.

oxide) production in both transgenic mice and non-transgenic mice, but the level of ROS production was greater in the OVX transgenic mice than in the OVX non-transgenic mice (Fig. 2). We next measured inflammatory cytokine levels in the liver. Ovariectomy significantly increased hepatic expression of IL-6 mRNA to the same degree in both transgenic mice and non-transgenic mice (Fig. 3). This ovariectomy-induced increase in hepatic IL-6 mRNA was consistent with the results of a previous report that OVX mice produced more hepatic

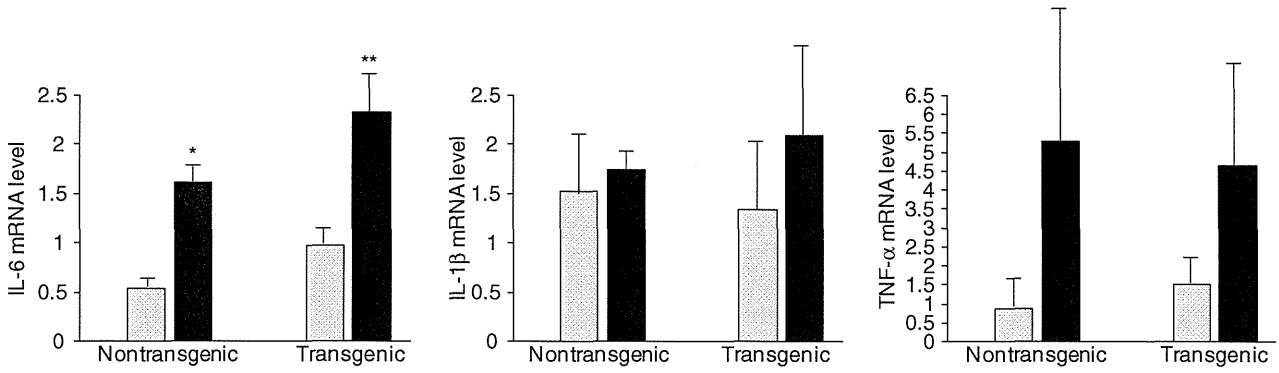

Figure 3 Expression levels of inflammatory cytokines in sham-operated and ovariectomized (OVX) FL-N/35 transgenic and non-transgenic mice. The mRNA levels of interleukin (IL)-6, IL-1β and tumor necrosis factor (TNF)-α were measured by real-time reverse transcription polymerase chain reaction for five mice in each group. The relative quantities of target mRNA in the liver were normalized with GAPDH mRNA. *$P < 0.05$ vs sham-operated non-transgenic mice. **$P < 0.05$ vs sham-operated transgenic mice. □, Sham; ■, OVX.

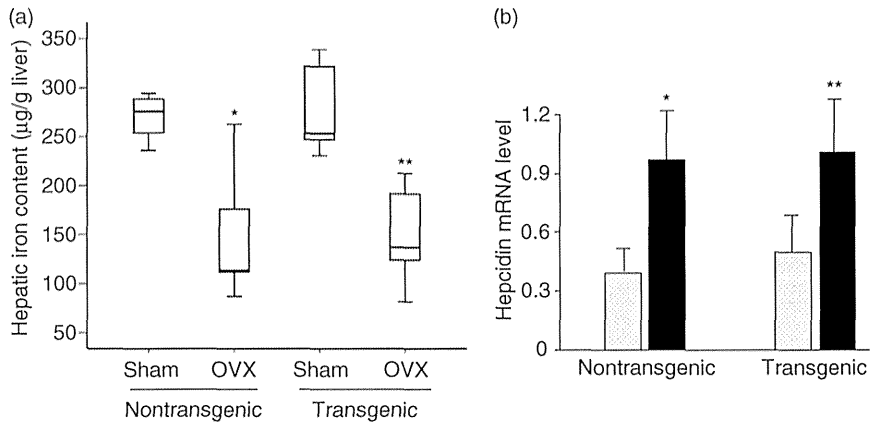

Figure 4 Hepatic iron content and hepcidin mRNA level in sham-operated and ovariectomized (OVX) FL-N/35 transgenic and non-transgenic mice. (a) Hepatic iron content in mice in each group ($n = 5$). The results are shown as box plot profiles. The bottom and top edges of the boxes are the 25th and 75th percentiles, respectively. Median values are shown by the line within each box. $^{*}P < 0.05$ vs sham-operated non-transgenic mice. $^{**}P < 0.05$ vs sham-operated transgenic mice. (b) The mRNA level of hepcidin was measured by real-time reverse transcription polymerase chain reaction for five mice in each group. The relative quantities of target mRNA in the liver were normalized with GAPDH mRNA. $^{*}P < 0.05$ vs sham-operated non-transgenic mice. $^{**}P < 0.05$ vs sham-operated transgenic mice. □, Sham; ■, OVX.

IL-6 than non-OVX mice after chemically induced liver injury.[5] There also was a trend for increase in TNF-α and IL-1β mRNA expression after ovariectomy in both the transgenic mice and non-transgenic mice, but their increases did not reach statistical significance, probably because of the large deviation (Fig. 3). These results suggested that inflammatory cytokines were unlikely to be associated with greater ROS production in OVX transgenic mice than in OVX non-transgenic mice.

Hepatic iron content and hepcidin expression level in the liver

We previously reported that male FL-N/35 transgenic mice developed hepatic iron accumulation through the reduced transcription of hepcidin,[18] a negative regulator in iron homeostasis.[21,22] Excess divalent iron can be highly toxic, mainly via the Fenton reaction producing hydroxyl radicals.[23] Therefore, we measured hepatic iron content to assess whether greater ROS production resulted from increased hepatic iron accumulation in OVX transgenic mice. Unexpectedly, ovariectomy significantly decreased hepatic iron content to the same degree in both transgenic mice and non-transgenic mice (Fig. 4a). These results are potentially explained by significantly increased transcription of hepcidin after ovariectomy (Fig. 4b). Ovariectomy-induced increase in hepatic IL-6 mRNA may in turn account for increased hepcidin transcription, because IL-6 acts to stimulate hepcidin expression through the STAT3 pathway.[24] These results suggested that hepatic iron content was not related to greater ROS production in OVX transgenic mice than in OVX non-transgenic mice.

Attenuated antioxidant potential against ovariectomy-induced ROS production in FL-N/35 transgenic mice

The increase in inflammatory cytokine production and the hepatic iron content after ovariectomy were comparable in transgenic and non-transgenic mice. Nevertheless, the serum ALT level, hepatic steatosis and ROS production were greater in OVX transgenic mice than in OVX non-transgenic mice. Therefore we measured dROM and BAP in serum to compare antioxidant potentials in OVX transgenic and OVX non-transgenic mice. We confirmed the significant negative correlation between the ratio of BAP to dROM and hepatic content of superoxide (Fig. 5). As expected, the values for dROM were higher in OVX mice than in sham-operated mice, regardless of whether they were transgenic or non-transgenic. However, a significant increase in the BAP value was found in OVX non-transgenic mice but not in OVX transgenic mice, which resulted in a lower ratio of BAP to dROM in the OVX transgenic mice than in the OVX non-transgenic mice (Table 2).

The first line of defense against ROS is the detoxifying enzymes that scavenge ROS. These include SOD and

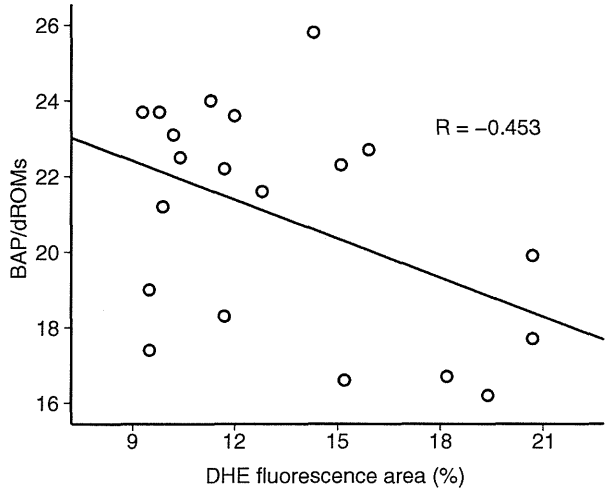

Figure 5 Negative correlation between the ratio of biological antioxidant potential (BAP) to derivatives of reactive oxygen metabolites (dROM) and hepatic content of superoxide. $R = -0.453$, $P < 0.05$. Hepatic content of superoxide was determined based on the area of dihydroethidium (DHE) fluorescence.

GPx1. Therefore we next investigated the expression levels of SOD2 and GPx1. The hepatic expression levels of SOD2 mRNA and GPx1 mRNA were significantly greater in OVX non-transgenic mice than in sham-operated non-transgenic mice, but were comparable in OVX transgenic mice and sham-operated transgenic mice (Fig. 6a). Western blot analysis of the hepatic mitochondria fractions also showed significant increases of SOD2 and GPx1 expression in OVX non-transgenic mice but not in OVX transgenic mice (Fig. 6b). These results suggested that antioxidant defense mechanisms may be induced against ovariectomy-related ROS production in non-transgenic mice but not in transgenic mice.

SIRT3 and PGC-1α expression in OVX FL-N/35 transgenic mice

Proliferator-activated receptor-γ co-activator-1α is a master regulator of mitochondrial biogenesis and respiration[25] and required for the induction of many ROS-detoxifying enzymes, including SOD2 and GPx1 upon oxidative stress.[26] SIRT3 is a member of a class III histone deacetylase and is reported to mediate PGC-1α-dependent induction of ROS-detoxifying enzymes.[27] In accordance with the changes in SOD2 and GPx1 levels after ovariectomy, the hepatic expression of SIRT3 mRNA was significantly greater in OVX non-transgenic mice than in sham-operated non-transgenic mice, but comparable in OVX transgenic mice and sham-operated transgenic mice (Fig. 7a). Western blot analysis of hepatic mitochondria showed a significant increase of SIRT3 expression in OVX non-transgenic mice but not in OVX transgenic mice (Fig. 7a).

Proliferator-activated receptor-γ co-activator-1α interacts with various nuclear receptors in addition to peroxisome proliferator-activated receptor-γ and is docked to the promoter of its target genes by all these nuclear receptors. Therefore, we investigated PGC-1α expression levels not only in liver homogenates but also in the nuclear fraction of mouse liver. The expression levels of PGC-1α in liver homogenates were comparable in sham-operated and OVX non-transgenic mice and in sham-operated and OVX transgenic mice. However, the expression levels of PGC-1α in the nuclear fraction of the liver significantly increased after ovariectomy in both non-transgenic and transgenic mice, and OVX transgenic mice had a lower PGC-1α expression level than OVX non-transgenic mice (Fig. 7b). These results suggested that the antioxidant potential against ovariectomy-induced ROS production may be reduced in OVX transgenic mice through lesser activation of PGC-1α than in OVX non-transgenic mice.

Table 2 Derivatives of reactive oxygen metabolites (dROM), biological antioxidant potential (BAP) and ratio of BAP to dROM

	Non-transgenic		Transgenic	
	Sham-operated	OVX	Sham-operated	OVX
dROM (U.CARR)	145.2 ± 15.1	158.7 ± 15.9*	170.8 ± 10.4	199.3 ± 21.1**
BAP (μmol/L)	3217 ± 123	3644 ± 177*	3362 ± 178	3542 ± 140
Ratio of BAP to dROM	22.3 ± 2.3	23.1 ± 2.0	20.8 ± 1.8	17.8 ± 1.9***

Data are mean ± standard deviation.
*$P < 0.05$ compared with sham-operated non-transgenic mice. **$P < 0.05$ compared with sham-operated transgenic mice. ***$P < 0.05$ compared with ovariectomized (OVX) non-transgenic mice.

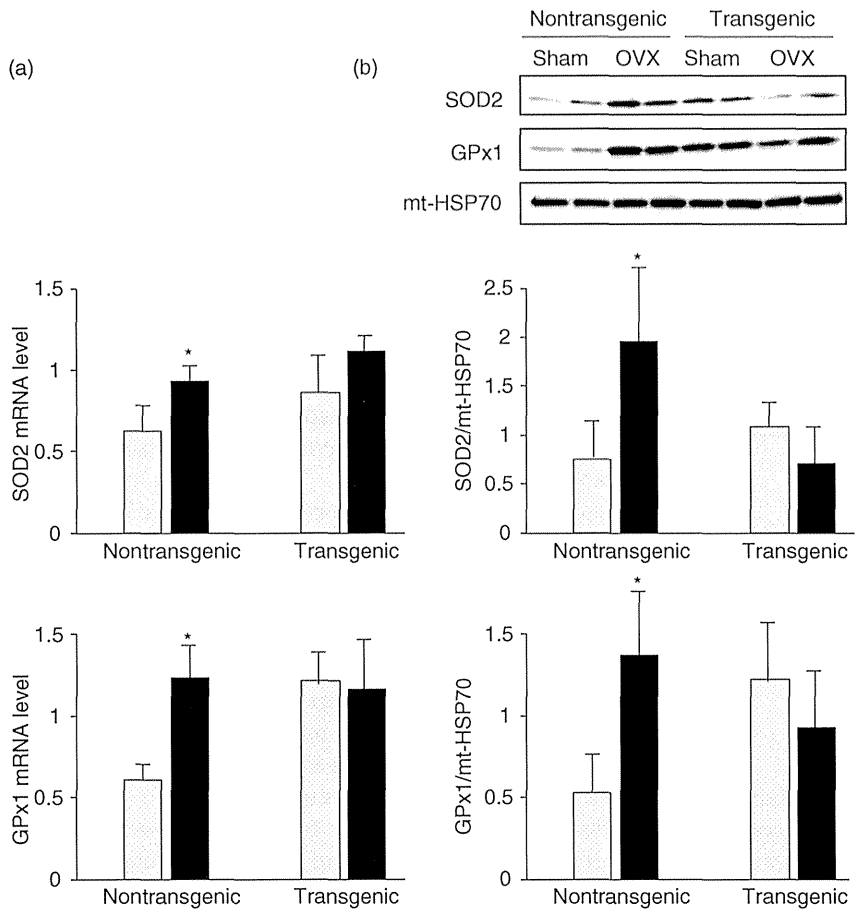

Figure 6 Expression levels of superoxide dismutase 2 (SOD2) and glutathione peroxidase 1 (GPx1) in sham-operated and ovariectomized (OVX) FL-N/35 transgenic and non-transgenic mice. (a) The mRNA levels of SOD2 and GPx1 were measured by real-time reverse transcription polymerase chain reaction for five mice in each group. The relative quantities of target mRNA in the liver were normalized with GAPDH mRNA. (b) Immunoblots for SOD2 and GPx1 were performed using mitochondrial fractions of liver lysates from five mice in each group. $^*P < 0.05$ vs sham-operated non-transgenic mice. □, Sham; ■, OVX.

Suppressed AMPK activation in OVX FL-N/35 transgenic mice

Proliferator-activated receptor-γ co-activator-1α activity is modulated through both transcriptional regulation and regulation of its activity by post-translational modifications.[28] AMPK is one of the signaling pathways regulating PGC-1α and acts both through modulation of PGC-1α transcription and by phosphorylation of the PGC-1α protein.[28] HCV has been shown to reduce the kinase activity of AMPK through Ser485/491 phosphorylation of AMPK.[29] Therefore, we examined the expression levels of AMPK to investigate the mechanisms underlying the lower PGC-1α expression in the nuclear fraction of the OVX transgenic liver. The expression levels of AMPKα, which is one of the three subunits (α, β and γ) of AMPK, were comparable in sham-operated and OVX mice and in non-transgenic and transgenic mice. However, the expression level of phosphorylated AMPKα was significantly greater in OVX non-transgenic mice than in mice in the three other groups, though it was similar in sham-operated transgenic mice and OVX transgenic mice (Fig. 7c). In addition, its levels were significantly greater in non-transgenic mice than in transgenic mice (Fig. 7c). These results suggested that AMPK was activated in OVX non-transgenic mice, but not in OVX transgenic mice, because AMPK is active only after phosphorylation of the α-subunit at a threonine residue within the kinase domain (T172) by upstream kinases.[30] Taken together, the results in the present study suggested that OVX FL-N/35 transgenic mice developed marked hepatic steatosis concomitant with increased ROS production via attenuation of antioxidant potential through inactivation of the AMPK/PGC-1α signaling pathway.

DISCUSSION

THE OVX MICE in the present study were assumed to be a standard model for evaluating the biological effect of ovariectomy because the effects of ovariectomy

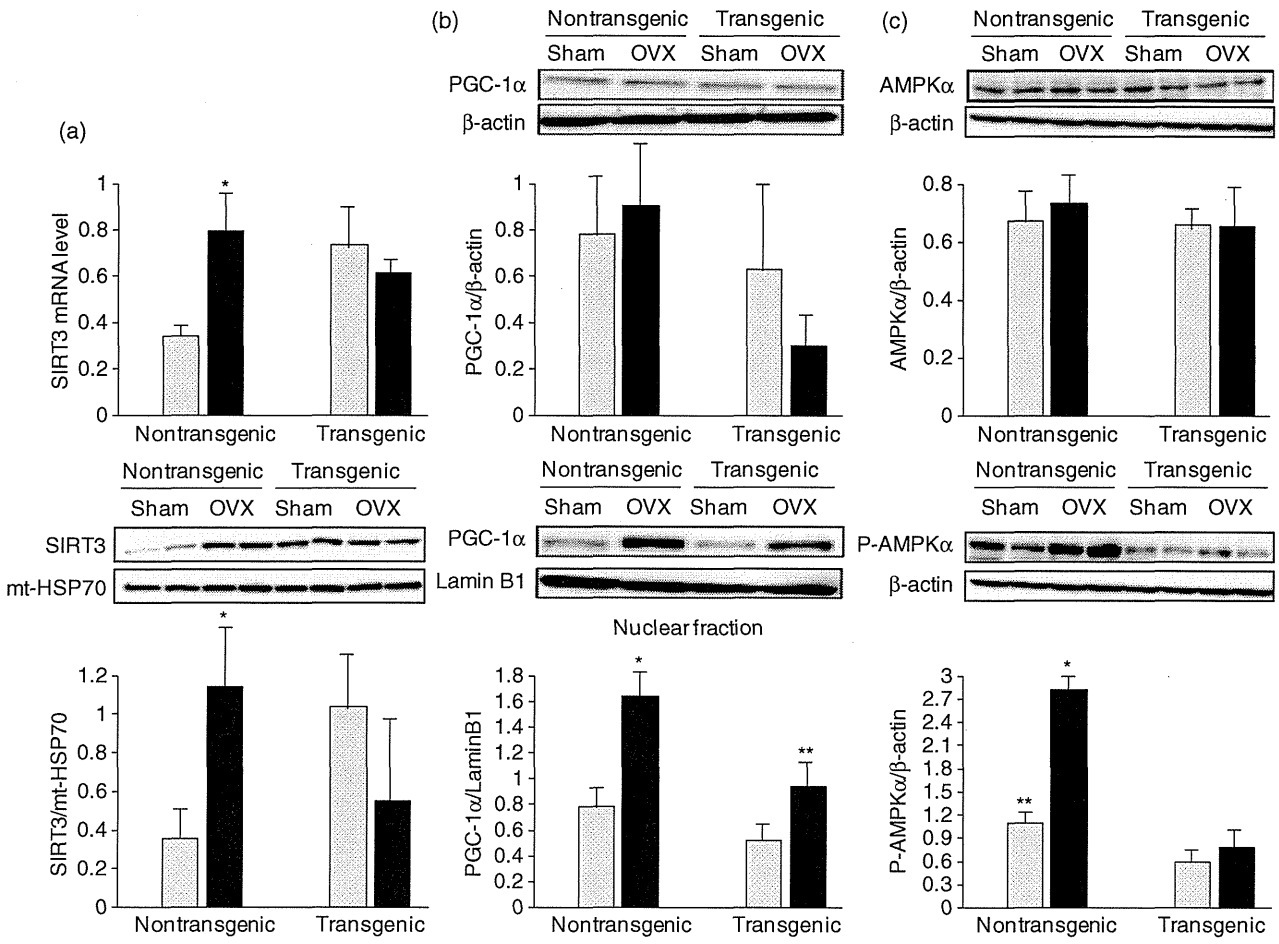

Figure 7 Expression levels of sirtuin 3 (SIRT3), peroxisome proliferator-activated receptor-γ co-activator-1α (PGC-1α), adenosine monophosphate-activated protein kinase α (AMPKα), and phosphorylated AMPKα (P-AMPKα) in sham-operated and ovariectomized (OVX) FL-N/35 transgenic and non-transgenic mice. (a) The mRNA levels of SIRT3 were measured by real-time reverse transcription polymerase chain reaction for five mice in each group. The relative quantities of target mRNA in the liver were normalized with GAPDH mRNA. Immunoblots for SIRT3 were performed using the mitochondrial fractions of liver lysates from five mice in each group. (b) Immunoblots for PGC-1α were performed using liver lysates and their nuclear fractions from five mice in each group. $*P < 0.05$ vs mice in the other three groups. $**P < 0.05$ vs sham-operated transgenic mice. (c) Immunoblots for AMPKα and P-AMPKα were performed using liver lysates from five mice in each group. $*P < 0.05$ vs mice in the other three groups. $**P < 0.05$ vs sham-operated transgenic mice. □, Sham; ■, OVX.

on dietary intake, bodyweight, uterine weight, liver weight and serum leptin levels were similar to the results from previous studies.[31–34] Ovariectomy increased ROS (superoxide) production in both transgenic liver and in non-transgenic liver, which was consistent with the ovariectomy-induced increase in NADPH oxidase activity[12] and the protective effect of estrogen against mitochondrial oxidative damage[13] found in previous studies. Of note was the much greater degree of ROS production after ovariectomy in transgenic mice than in non-transgenic mice. These results suggested that HCV protein expression has the potential to increase the sensitivity to oxidative stress in the liver. At least two possibilities may account for the increased sensitivity to oxidative stress in FL-N/35 transgenic mice. One possibility is an additive effect of HCV-induced ROS production on ovariectomy-induced oxidative stress. The HCV core protein has been shown to inhibit mitochondrial electron transport[35] and to induce ROS production.[36] In fact, basal ROS production tended to be higher in